Astron. Astrophys. 339, 629–637 (1998)

ASTRONOMY AND ASTROPHYSICS

Kelvin-Helmholtz instability of stratified jets

II. The nonrelativistic limit

M. Hanasz[1,2] **and H. Sol**[1]

[1] DARC, UPR176 du CNRS, Observatoire de Paris-Meudon, 5 Place J. Janssen, F-92195 Meudon Cedex, France
[2] Toruń Centre for Astronomy, Nicolaus Copernicus University, PL-87-148 Piwnice/Toruń, Poland (mhanasz@astri.uni.torun.pl; sol@obspm.fr)

Received 15 May 1998 / Accepted 3 September 1998

Abstract. In this paper we continue investigations of the Kelvin-Helmholtz instability of stratified jets. We first generalize our previous analytical results by taking into consideration relativistic motion and relativistic equation of states for the three components namely the inner beam, the sheet or envelope and the ambient medium, and derive the dispersion relation for the Kelvin-Helmholtz instability. The ultrarelativistic limit of paper I as well as the nonrelativistic limit for both the equations of state and the jet bulk speed can be deduced. Exploring a wider range of parameters, we find evidence for two main types of instability modes, with mode crossing and interaction between modes. These two modes correspond to the excitation of sound waves in the beam and in the envelope which can both act as a resonant wave guide. As a result, the addition of an inner beam inside a jet can strongly enhance the linear growth of its Kelvin-Helmholtz instability. The stratified jet scenario appears quite relevant to give account for the complex morphology and velocity fields now observed in a few jets such as in M87, where various layers with respect to the jet axis are clearly visible.

Key words: galaxies: jets – hydrodynamics – instabilities

1. Introduction

In the former paper of this series (Hanasz and Sol , hereafter Paper I) we investigated the Kelvin-Helmholtz instability of stratified jets made of an inner relativistic beam surrounded by a slow moving envelope, embedded in an external medium. In the case of relativistic motion of the inner component ("beam" or "core") close to the line of sight, it is natural to expect that it is the one which is better visible to the observer due to the relativistic beaming of the emitted radiation. Our aim in Paper I was indeed to answer the question how the presence of a surrounding envelope can change the stability properties of the inner relativistic component. However the question can be put the other way around, how does the presence of an inner faster component modify the Kelvin-Helmoltz instability of an astrophysical nonrelativistic jet. Such a scenario appears quite reasonable since the inner component can be accelerated by a different physical mechanism than the outer one and can have different properties regarding composition, velocity, electromagnetic emission. Several cases applying to different astrophysical objects are of interest since the fast and the slow components can be relativistic or non-relativistic gases and can have any kind of bulk velocities.

Extragalactic jets, which first motivated our analysis, provide several examples of relativistic and non-relativistic cases with an inner fast beam likely surrounded by a slow envelope. They are discussed in details in paper I. The jet of 3C273 for instance has been described as a fast-moving inner jet within a slow-moving cocoon (Bahcall et al, 1995). The jet of M87 also shows various layers with differing properties (Biretta, 1996). More generally the new technics of tomography of the synchrotron radio sources developed by Rudnick and Katz-Stone (1996) shows the presence of coaxial features with distinct spectral and polarization properties and wider than jets themselves in a number of sources. Such envelopes could be due either to the growth of boundary or entrainment layers, to the remnant of earlier jets, or to secondary flows ejected from the central engine. Indeed several scenarios offer the possibility to expel low speed outflows from accretion disks. Such a situation naturally occurs for instance when the surface of the disk is so hot that particles reach the escape velocity, as considered in the X-ray Compton heating model (Begelman, Mc Kee, 1983) or if broad emission lines come from magnetically confined clouds associated to molecular gas flowing out as a wind reaching speeds of a few thousand km/s from the outer parts of accretion disks (Emmering et al, 1992). Broad absorption lines (BAL) also provide observational evidence for slow outflows at about $10^4 - 3 \times 10^4$ km/s in QSO (although usually radio-quiet ones) and at about 10^3 km/s in 50% of Seyfert AGN. The warm absorber seen in X-rays in 50% of Seyfert AGN and in a few QSO is another example of a gas in motion close to the central engine. The presence of accretion disks, rotation and magnetic fields suggest that collimation of such outflows is likely to occur at some level. The slow-moving gas of these outflows can then be interpreted as a slow outer envelope of the jet, the whole configuration being described by a "stratified" core-sheath scenario. Observational support to this view is provided by recent spectroscopic data by the HST of the nuclear region of the Seyfert galaxy NGC

Send offprint requests to: M. Hanasz

4151 which revealed the probable outflow at about 350 km/s of narrow lines emitting clouds within a biconical region about the nucleus centered on the radio axis (Hutching et al, 1998). This may be an example of extragalactic stratified jet where the inner beam is better described in the non-relativistic limit.

Several cases of stellar jets can also be described by the non-relativistic core-sheath jet model. First of all, the analysis of the kinematical properties of jets and outflows from young stellar objects (YSO) revealed by spectroscopic and proper motion data shows the existence of a complex velocity field with the presence of components at different speed along the main jet axis (Padman et al, 1991; Reipurth, Heathcote, 1993; Ray, Mundt, 1993; Stahler, 1993; Solf, 1997; et al, 1997). High and low velocity gas components, "jets" and "outflows", can be interpreted in different ways. The jets may drive the outflows by entrainment of the surrounding medium (Stahler, 1993; Hartigan et al, 1993; Guilloteau et al, 1997). However, other kinds of scenario consider the possibility that two types of wind are indeed ejected from the central source, one from the star and its magnetosphere, and one from the disk. Such a proposal came out for the jets issued from T Tauri stars from the analysis of forbidden line emission (Kwan, Tademaru, 1988; Kwan, 1997). The possible occurrence of X-winds from young stellar objects (Shu et al, 1994; Shu, Shang, 1997; Ferreira et al, 1997) provides as well theoretical arguments for the existence of different types of outflows in these sources (stellar wind, coronal wind, X-wind, disk wind), likely leading to the presence of several interfaces between matter flowing at different velocities. Evidences for such a situation come also from recent numerical simulation of jet formation which consider the interaction between the central magnetosphere and the accretion disk. Both in the classical limit of young stellar objects (Goodson et al, 1997) and in the general relativistic limit of active galactic nuclei (Koide et al, 1998), a two-component outflow arises, with the formation of a fast inner well-collimated jets and a slow outer jet. Although the physical explanation of these phenomena can be different depending on the detailed considered frame, the general occurrence of stratified jets with several layers appears well established.

Besides young stellar objects, a number of protoplanetary and planetary nebulae host bipolar outflows with a velocity of a few hundreds of km/s, ten times higher than the typical expansion velocity of the nebulae (Solf, 1993; Corradi, Schwarz, 1993a) which can be described as an inner beam propagating into a slow-moving envelope. Indeed spectacular examples of highly collimated outflows have been recently found in CRL2688, the Egg nebula, and in M2-9 (Sahai et al, 1998a, 1998b; Schwarz et al, 1997; Balick et al, 1998). In CRL2688, a sharp interface is seen in the infrared between the high speed jet-like features which produce polar cavities and the surrounding slow outflow of the extended nebula. M2-9 has fast, supersonic, highly collimated outflows reaching a total extent of about 0.4 pc and a speed exceeding 300 km/s. The structure of this bipolar or "butterfly" nebula is very symmetrical with features mirrored on the opposite side of the star and suggest coaxial stratification of the outflow. Formation of such outflows may be rather analogous to usual models for other astrophysical jets since the central stellar system, a very close pair, is believed to have generate a disk (possibly observed by HST) which acts as a nozzle and collimates into jets the high speed wind from one of the central stars. Generally speaking, the various types of planetary nebulae are ascribed to interaction of stellar winds at different speeds, fast winds sweeping into older slower ones. Jets are sometimes observed along the polar axis as well as FLIERS (fast low-ionization emission regions) with highly supersonic speed of about 50 km/s (Corradi, Schwarz, 1993b; Balick et al, 1994; Hajian et al, 1997). It is clear that outflows at different speeds are present in all these types of objects, and collimation in a part of them for which the stratified jet scenario we are studying may be of some interest.

In this paper, we first write the general dispersion relation for the Kelvin- Helmholtz instability of a general case of relativistic core-sheet astrophysical jets. Then we investigate in more details the case where both the inner (core or beam) and outer (sheet or envelope) components are non-relativistic. This non- relativistic limit was not analyzed in paper I, although it can be relevant for both stellar and extragalactic jets, as well as for laboratory jets. As in paper I, we assume a 2-dimensional slab geometry for the jet. Transition layers at all interfaces are described within the vortex-sheet approximation. Pinching and helical perturbations of cylindrical jets can then be related to symmetrical and antisymmetrical perturbations of the slab jet. Only high order fluting modes of cylindrical jets do not have counterparts in slab jets (Ferrari et al, 1982; Hardee, Norman, 1988). We consider a core-sheet jet made of three layers (see Fig. 1 of Paper I) and analyze the temporal behavior of its Kelvin-Helmholtz instability at the linear stage.

2. Description of the problem

2.1. The thermodynamical relations

In the following we shall apply the equation of state of the form

$$p\rho_r^{-\Gamma} = \text{const}, \tag{1}$$

where $\rho_r \equiv mn$ is the rest mass density. The rest frame density of the gas is

$$\rho = \rho_r(1+\epsilon), \tag{2}$$

where ϵ is the specific internal energy, which is related to the pressure by the following relation

$$p = (\Gamma - 1)\epsilon\rho_r c^2 \tag{3}$$

The enthalpy and the sound speed are respectively

$$w = \rho + \frac{p}{c^2}, \tag{4}$$

$$c_s^2 = \frac{\Gamma p}{w}. \tag{5}$$

2.2. Basic definitions

As in Paper I we assume that a jet flows along the x-axis in the Cartesian reference frame $x-z$. The unperturbed equilibrium state is characterized by the core radius R_c, sheet radius R_s, velocities V_{oc} (V_{os}, V_{oe}) and densities ρ_{oc} (ρ_{os}, ρ_{oe}) of the core (sheet and external medium). Since the configuration is assumed to be in pressure equilibrium,

$$p_o \equiv p_{oc} = p_{os} = p_{oe}. \tag{6}$$

The relevant equations can be transformed to the dimensionless form by the introduction of dimensionless quantities. In contrast to the former paper we will not introduce the density contrasts, but instead the enthalpy contrasts, in order to obtain the dispersion relation in a form which is the same for ultra- and non-relativistic limits. We define the enthalpy contrasts as

$$\eta_{nm} = \frac{w_{no}}{w_{mo}}, \tag{7}$$

where $n, m = c, s, e$ and the index "o" stands for unperturbed zero-order values of enthalpy. In the ultra-relativistic limit the relation between η_{cs} and the density contrast used in Paper I is $\eta_{cs} = \Gamma_c \nu_s$ (please note typing errors in figure captions of Paper I where 'ν_c' and 'ν_s' should be replaced by 'ν_s' and 'ν_e' respectively). The relations between sound speeds of different components are given by

$$\frac{c^2_{sno}}{c^2_{smo}} = \frac{\Gamma_n \eta_{nm}}{\Gamma_m} \tag{8}$$

The Mach numbers of the components are

$$M_n = \frac{V_{no}}{c_{sno}}, \tag{9}$$

where c_{sn} ($n = c, s, e$) are the sound speeds of each medium. Without loss of generality we can assume that $M_e = 0$.

2.3. Equations of motion

For the sake of generality we shall apply relativistic equations of motion (Ferrari et al. 1978, Paper I) for all the components

$$\gamma_n^2\Big(\rho_n+\frac{p_n}{c^2}\Big)\left[\frac{\partial \boldsymbol{V}_n}{\partial t}+(\boldsymbol{V}_n\cdot\boldsymbol{\nabla})\boldsymbol{V}_n\right]+\boldsymbol{\nabla}p_n+\frac{\boldsymbol{V}_n}{c^2}\frac{\partial p_n}{\partial t}=0, \tag{10}$$

$$\gamma_n\left(\frac{\partial \rho_n}{\partial t}+\boldsymbol{V}_n\boldsymbol{\nabla}\rho_n\right)+\Big(\rho_n+\frac{p_n}{c^2}\Big)\left[\frac{\partial \gamma}{\partial t}+\boldsymbol{\nabla}(\gamma \boldsymbol{V}_n)\right]=0. \tag{11}$$

The system of equations describing independently each fluid should be closed by the appropriate matching conditions at all the fluid interfaces and by the requirement that the magnitude of the perturbations vanish at $z \to \infty$, (the Sommerfeld radiation condition) or equivalently, that only outgoing waves in the external medium are considered.

The matching conditions state that pressures (p) and transversal displacements (h) of fluids should be equal on both sides of each interface, namely at the internal interface ($z = R_c$)

$$p_c = p_s, \quad h_c = h_s, \tag{12}$$

and at the internal interface ($z = R_s$)

$$p_s = p_e, \quad h_s = h_e. \tag{13}$$

2.4. The linear solutions

As in Paper I, we introduce dimensionless quantities with spatial coordinates scaled to R_c , time scaled to R_c/c_{sco}, pressures in all the media scaled to p_0 and velocities to the sound speeds of the core. We introduce the parameter $R = R_s/R_c$ as the dimensionless sheet radius.

After the linearization of the system of equations we substitute perturbations of the form

$$\delta'_{c,s} = [\delta^+_{c,s} F^+_{c,s}(z) + \delta^-_{c,s} F^-_{c,s}(z)] \exp i(k_\| x - \omega t) + c.c. \tag{14}$$

with $F^\pm_{c,s}(z) = \exp(\pm i\, k_{c,s\perp} z)$ to describe waves propagating in positive and negative z-directions in the core and in the sheet. Here we use $k_{||}$ and $k_{c,s,e\perp}$ for longitudinal and transverse wavenumbers (instead of k_x and k_{c,s,e_z} used in Paper I). Perturbations in the external medium are of the form

$$\delta'_e = \delta^+_e F^+_e(z) \exp\, i(k_\| x - \omega t) + c.c. \tag{15}$$

with $F^+_e(z) = \exp\, i\, k_{e\perp} z$ and only outgoing waves (for $z > 0$). In the temporal stability analysis, the parallel wavenumber, $k_\|$, is real and the frequency, ω, complex. The (complex) transverse wavenumbers in the core, sheet, and external regions are

$$k_{c\perp} = \left(\omega^2_{co} - k^2_{co\|}\right)^{1/2} \tag{16}$$

$$k_{s\perp} = \left(\frac{\Gamma_c}{\eta_{cs}\Gamma_s}\omega^2_{so} - k^2_{so\|}\right)^{1/2} \tag{17}$$

$$k_{e\perp} = \left(\frac{\Gamma_c}{\eta_{cs}\eta_{se}\Gamma_e}\omega^2 - k^2_\|\right)^{1/2} \tag{18}$$

where

$$\omega_{co} = \gamma_c(\omega - M_c k_\|), \tag{19}$$

$$k_{co\|} = \gamma_c(k_\| - \beta^2_{sco} M_c \omega), \tag{20}$$

$$\omega_{so} = \gamma_s(\omega - \sqrt{\eta_{cs}\Gamma_s/\Gamma_c} M_s k_\|), \tag{21}$$

$$k_{so\|} = \gamma_s(k_\| - \sqrt{\eta_{cs}\Gamma_s/\Gamma_c}\beta^2_{sco} M_s \omega), \tag{22}$$

are respectively the frequencies in the rest frames of core and sheet fluids and

$$\gamma_c = (1 - \beta^2_{sco} M^2_c)^{-1/2}, \tag{23}$$

$$\gamma_s = (1 - (\eta_{cs}\Gamma_s/\Gamma_c)\beta^2_{sco} M^2_s)^{-1/2}, \tag{24}$$

$$\beta^2_{sco} = \frac{\Gamma_c(\Gamma_c - 1)\epsilon_c}{1 + \Gamma_c \epsilon_c} \tag{25}$$

are the core and sheet Lorentz factors and β_{sco} is the ratio of core sound speed to the speed of light.

2.5. The dispersion relation

Following the way presented in Paper I we arrive at the dispersion relation

$$\frac{Z_s}{Z_c}\left[\frac{1+\mathcal{R}_{se}e^{2ik_{s\perp}(R-1)}}{1-\mathcal{R}_{se}e^{2ik_{s\perp}(R-1)}}\right]=\begin{cases}\coth ik_{c\perp} & \text{for } \varepsilon=1\\ & \text{or}\\ \text{th } ik_{c\perp} & \text{for } \varepsilon=-1\end{cases} \quad (26)$$

where $\varepsilon = 1$ corresponds to symmetric and $\varepsilon = -1$ to the antisymmetric solutions. This relation appears to be of the same structure, in the currently considered general case, as the one derived in Paper I for the case of a relativistic inner core. There are however differences in the shapes of some involved quantities defined by the formulae (16-25). The minor differences follow from the more general equations of state and the Lorentz transformation of ω and $k_\parallel$ for the sheet component.

The relevant reflection coefficients at core-sheet (for the waves incident from the core side), sheet-core and sheet-external gas interfaces (for the waves incident from the sheet side) are respectively

$$\mathcal{R}_{cs} = \frac{Z_s - Z_c}{Z_s + Z_c}, \quad (27)$$

$$\mathcal{R}_{sc} = \frac{-1}{\mathcal{R}_{cs}}, \quad (28)$$

$$\mathcal{R}_{se} = \frac{Z_e - Z_s}{Z_e + Z_s}, \quad (29)$$

where

$$Z_c = \omega_{c_0}^2/k_{c\perp}, \quad (30)$$

$$Z_s = \omega_{s_0}^2/(\eta_{cs}k_{s\perp}), \quad (31)$$

$$Z_e = \omega^2/(\eta_{cs}\eta_{se}k_{e\perp}). \quad (32)$$

are the complex normal acoustic impedances for the core, sheet and external medium, which are defined with the accuracy to a factor constant across all the components (eg. the expressions for $Z_{c,s,e}$ would be identical with the analogous expressions of Paper I after the multiplication by Γ_c). As noticed in Paper I the dispersion relation (26) converges to the case of single jet without sheet for $R = 1$, and to the case of single jet with infinite sheet for $R >> 1$.

2.6. The non-relativistic limit

To study the non-relativistic limit we assume that both the gases of sheet and core move with non-relativistic bulk velocities ($\gamma_c = \gamma_s = 1$), and that all the three components are described by non relativistic equations of state with adiabatic indices $\Gamma_n = 5/3$ and the specific internal energies $\epsilon_n \to 0$. Then, from (25) it follows that $\beta_{sco}^2 \to 0$ and the relations between wavenumbers and frequencies in the core and sheet (19-22) reduce to

$$\omega_{co} = \omega - M_c k_\parallel, \quad (33)$$

$$k_{co\parallel} = k_\parallel, \quad (34)$$

$$\omega_{so} = \omega - \sqrt{\eta_{cs}\Gamma_s/\Gamma_c}M_s k_\parallel, \quad (35)$$

$$k_{so\parallel} = k_\parallel, \quad (36)$$

These relations can be taken into account in (16-18), (30-32) and (29) to obtain the non-relativistic limit of the dispersion relation (26).

2.7. Limits of applicability of ultra-relativistic and non-relativistic equations of state

The dispersion relation (26) allows to examine a wide range of configurations of stratified jets including relativistic and non-relativistic bulk speeds as well as relativistic and non-relativistic equations of state for each component. One limiting case of relativistic bulk motion and ultra-relativistic equation of state for the core and non-relativistic sheet and external medium has been considered in Paper I. The present formulation of the problem comprises the previously studied limiting case and allows to specify its limits of applicability. The choice of relativistically hot core and non-relativistic sheet means that the internal energy is much larger than the rest energy of gas particles in the core and much smaller in the sheet. From Synge (1957), who gives the sound speed for the relativistic Synge gas versus temperature, we see that the non-relativistic adiabatic equation of state can be applied up to specific internal energies $\epsilon \sim 0.1$ and that the ultra-relativistic description starts to be valid above $\epsilon = 1$. In both the cases the sound speeds resulting from non-relativistic and ultra-relativistic equations of state do not depart from the values computed for the Synge gas by more then ~ 10 %.

3. Numerical solutions

The method used to solve the dispersion relation (26) in the non-relativistic limit is based on the Newton-Raphson method (Press et al. 1992) as in Paper I, but now the algorithm is more sophisticated. In the present approach we search for solutions for each $k_{\parallel n}$ independently on the one found for $k_{\parallel n-1}$, taking random values of (ω_r, ω_i) as the starting points for the Newton-Raphson method. This procedure does not require any *a priori* knowledge on the solutions, which are to be found. The results obtained in this way can be incomplete, ie. if there exist multiple modes of instability for a given $k_{\parallel n}$, not all of them are reached, but iterating the procedure for subsequent values of $k_{\parallel n}$ implies that all the modes are represented by more or less numerous points. In the next step we extend these solutions from the mentioned points downward and upward the k-axis applying first a linear extrapolation of (ω_r, ω_i) from $k_{\parallel n}$ to $k_{\parallel n+1}$ and then improving iteratively the extrapolated value with the Newton-Raphson method.

An exemplary numerical (antisymmetric) solution of the dispersion relation (26) is found for the following parameters of non-relativistic stratified jet: $M_c = 10$, $M_s = 3$, $\eta_{cs} = 1$, $\eta_{se} = 0.1$. The results are presented in Fig. 1, where we display the frequency ω_r and growth rate ω_i for $R = 1.75$, 2 and 5. Individual solutions are represented by points, which are

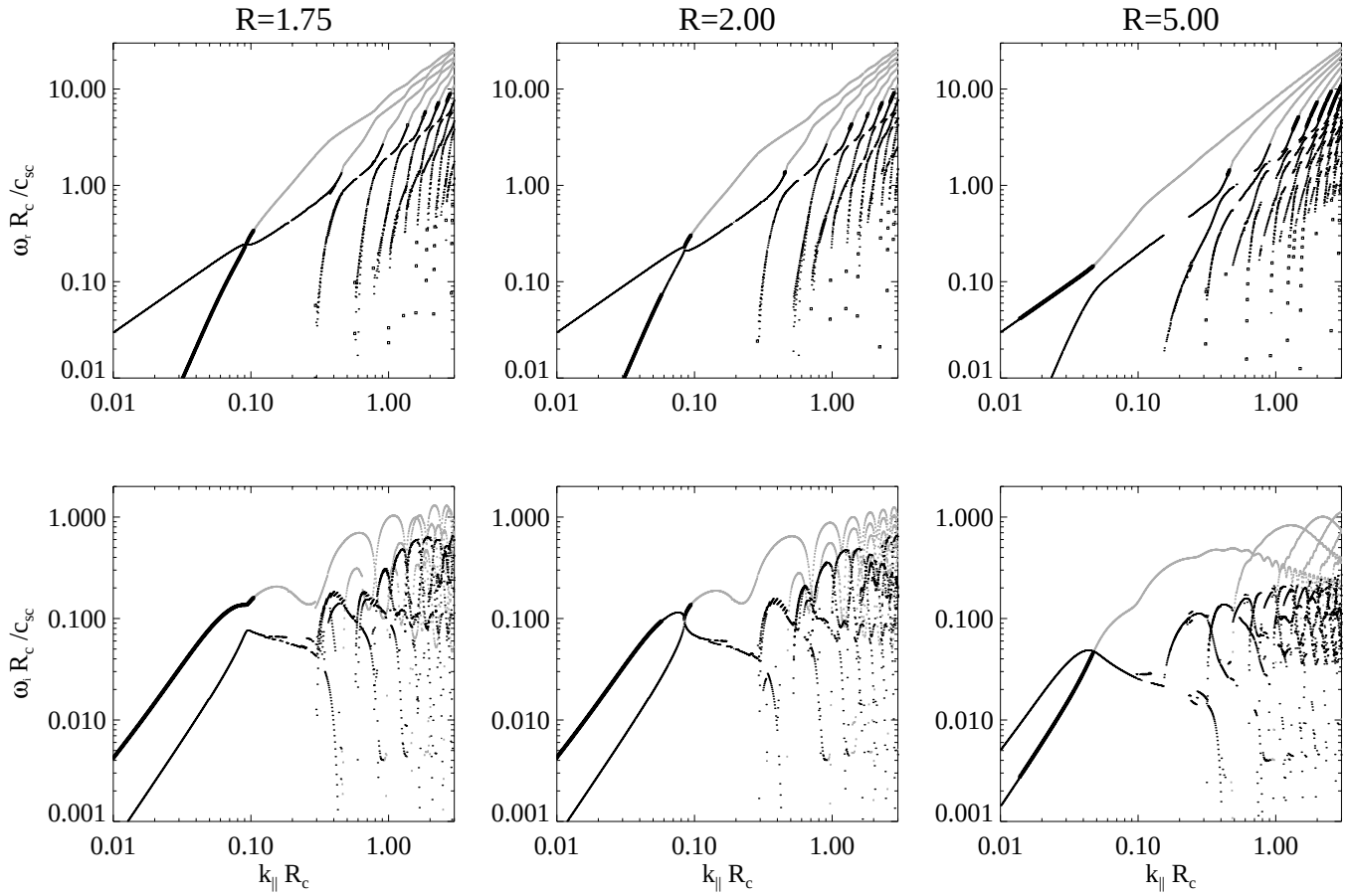

Fig. 1. The dependence of the frequency ω_r (upper panels) and growth rate ω_i (lower panels) on the longitudinal wavenumber k for antisymmetric solutions found for $M_c = 10$, $M_s = 3$, $\eta_{cs} = 1$, $\eta_{se} = 0.1$. Subsequent columns represent different values of R. The different types of lines are described in the text.

usually (but not everywhere) dense enough to form lines. As it is apparent, modes of different types are displayed simultaneously.

3.1. Classification of instability modes

It has been demonstrated by Payne and Cohn (1985) that at short and intermediate wavelengths the Kelvin-Helmholtz instability in supersonic jets has its origin in the fact that the internal sound waves are amplified ie. over-reflected at the supersonic jet's boundary. In the case of stratified jets, one should consider reflection of sound waves internal to the core at *cs*-boundary with the reflection coefficient $\mathcal{R}_{cs}$, reflection of sound waves internal to the sheet at the *sc*-boundary with $\mathcal{R}_{sc}$ and reflection of sound waves internal to the sheet at the *se*-boundary with $\mathcal{R}_{se}$. Computing the three reflection coefficients according to formulae (27), (28) and (29), for the numerical solutions of the dispersion relation (26), we find the following cases, which are distinguished in Fig. 1 in the way indicated below,

(a) $|\mathcal{R}_{cs}| > 1$, ($|\mathcal{R}_{sc}| < 1$) and $|\mathcal{R}_{se}| \leq 1$ (grey lines and points)
(b) $|\mathcal{R}_{cs}| \leq 1$, ($|\mathcal{R}_{sc}| \geq 1$) and $|\mathcal{R}_{se}| \leq 1$ (black-thick lines and points)
(c) $|\mathcal{R}_{cs}| \leq 1$, ($|\mathcal{R}_{sc}| \geq 1$) and $|\mathcal{R}_{se}| > 1$ (black-thin lines and points)
(d) $|\mathcal{R}_{cs}| > 1$, ($|\mathcal{R}_{sc}| < 1$) and $|\mathcal{R}_{se}| > 1$ (not present for the parameter set of Fig. 1.)

We note that while the case (a) has been already examined in Paper I, the cases (b), (c) and (d) represent new solutions specific to the Kelvin-Helmholtz instability in stratified jets. Let us note that in the case (a) the sound waves internal to the core are exclusively amplified, while their counterparts in the sheet and external medium are not. The set of solutions representing the case (a) will be called the *core modes*. In the case (c) the sound waves internal to the sheet are exclusively amplified on both the (*sc*) and (*se*) interfaces. The set of solutions of this type will be referred to as *sheet modes*. In addition, there are solutions with various properties corresponding to case (b), with wave amplification only on the *(sc)* interface, and to case (d) where the sound waves internal to the core as well as their counterpart internal to the sheet are amplified.

The different types of modes are in our classification well separated on the frequency diagrams. The core modes correspond to higher frequencies and higher typical growth rates for a fixed value of the wavenumber k. They have been widely described and discussed in Paper I, with their oscillating patterns

of growth rate around the limiting case of infinite sheet thickness (the limiting solutions for $R = 1$ and $R = \infty$ are not drown in Fig. 1). Here we will analyze in more details the sheet modes.

3.2. Wave amplification on sheet interfaces

The sheet modes can be interestingly compared to the case of a single jet composed of only the sheet with $M_s = 3$ and $\eta_{se} = 0.1$ embedded in an external medium, as illustrated in Fig. 2. Note, that now the scaling of the growth rate and the wavenumber is for subsequent panels modified with respect to Fig. 1. The scaling, based on the sheet radius R_s and the sheet sound speed c_{ss} is now adopted in order to keep the single jet solutions in the same position in different panels. We note the following two distinct effects: (1) The subsequent modes of the sheet branch are globally shifted toward smaller wavenumbers with respect to the fundamental and reflection modes of the single sheet-jet. This shift holds in such a way that the lines of maxima of both the sheet branch and the single jet solutions coincide on the growth rate diagrams. This is a signature of the fact that the sheet modes are indeed related to the sheet component. (2) We can also notice that the mentioned line of maxima changes its position with respect to the core modes on the growth rate diagrams depending on R.

We can see that the growth rates for the core modes and the corresponding wavenumbers grow with the growth of R in the sheet scaling applied in Fig. 2 or alternatively, the growth rates for the sheet modes and the corresponding wavenumbers diminish with the growth of R in the core scaling applied in Fig. 1. To explain this property let us note that the relation between the dimensionless quantities in the two scalings are $(k_{\|} R_s) = R \cdot (k_{\|} R_c)$ and $(\omega_i R_s / c_{ss}) = R c_{sc}/c_{ss} \cdot (\omega_i R_c / c_{sc})$. In addition we note that the core modes, which are similar to the single core-sheet single jet solutions, are expected be fixed in the core scaling. The sheet modes, which are not very different than the sheet-external single jet solutions, should be approximately fixed in the sheet scaling.

Another effect, well visible when looking at the growth rate diagram for $R = 5$ (Fig. 1), especially in the range of smaller wavenumbers, is that while the core modes are continuous and complete, the sheet modes are rather sparse even though we engaged a substantial effort in the process of making these solutions more complete. One can notice, however, that the corresponding lines on the frequency diagram are discontinuous, but much more regular. There is also a subtle structure resembling "hair" in the growth rate diagram for the first two reflection modes of the sheet type. Such microstructures or splitting of the sheet modes as well as the global shift towards larger wavelengths (effect (1)) denote the influence of the additional inner fast beam on the proper mode of the sheet.

Paper I was conversely devoted to the study of the effect of the sheet on the beam instability, and finally reduced to the analysis of the beam mode alone. We noted that variations of the sheet Mach number M_s do not significantly change the solutions with respect to the case $M_s = 0$. However, the range of variations of M_s was relatively narrow, from 0 to 3. In addition the numerical algorithm was rather designed to trace a single (fundamental or reflection) mode, then to search for new modes. Due to these circumstances we overlooked the presence of sheet modes. This is now evident that the sheet modes exist also for the stratified jets with relativistic cores, with appearance depending on the specific choice of parameters but qualitatively similar to the non-relativistic case described in the present paper.

3.3. Relation between modes

In the range of longer wavelengths (k below the values typical for reflection modes) we can notice the presence of two modes, which is in contrast to the single jet case, where in the mentioned range only the fundamental mode exists. In addition, varying the sheet radius as in Fig. 1 from smaller to larger values, we note that these two modes merge for $R \simeq 2$ and then connect in a different way, with a complex behavior of the growth rates and of the reflection coefficients. For $R \simeq 2$, the two modes crossing for the real part of their frequencies also coincide for their growth rates. So there is an exact crossing of eigenvalues, which can then no more be uniquely attached to a particular mode. This corresponds to a resonance between the two modes and allows coupling between them. The existence of mode crossing suggests that different types of coupling and interaction between modes can occur (Glatzel 1989).

It is a characteristic feature of the obtained solutions that the transition between the different modes is continuous. This is clearly illustrated by one branch on the $R = 5$ frequency diagram, which is the fundamental mode of the core (case (a)) at large wavenumbers, and subsequently case (b) and then case (c) of the sheet mode for smaller wavenumbers. The same is seen for the reflection modes, where the transition between the mode types does not coincide with gaps in solutions. The solutions of type (b) for the reflection modes are not seen on the growth rate diagrams because they are much below the lower limit of the vertical scale. On the different branches of Fig. 1, case (b) appears as transition solutions between core and sheet modes.

3.4. Wave propagation

Indeed, our classification of modes can be related to the longitudinal phase speed $v_{ph} = \omega_r / k_{\|}$ of modes. Case (a) corresponds to perturbations which propagate along the jet faster than sheet bulk velocity. At small wavelengths, waves associated to these core modes have indeed a longitudinal phase velocity smaller but approaching the bulk core velocity. Case (c) corresponds to perturbation propagating slower than sheet. Case (b) includes two main types of solutions. One at low frequency ω_r is already present in single core jet, with longitudinal phase velocity equal to zero or close to zero. The other one, at higher ω_r, appears for stratified jets, with a phase velocity equal or close to the sheet speed. They correspond respectively to standing or subsonic waves in the external medium and in the sheet.

An interesting property of the solutions in the range of longer wavelengths is such that one of the two modes ((b) or (c)) existing there represents non-dispersive waves (see Payne and Cohn

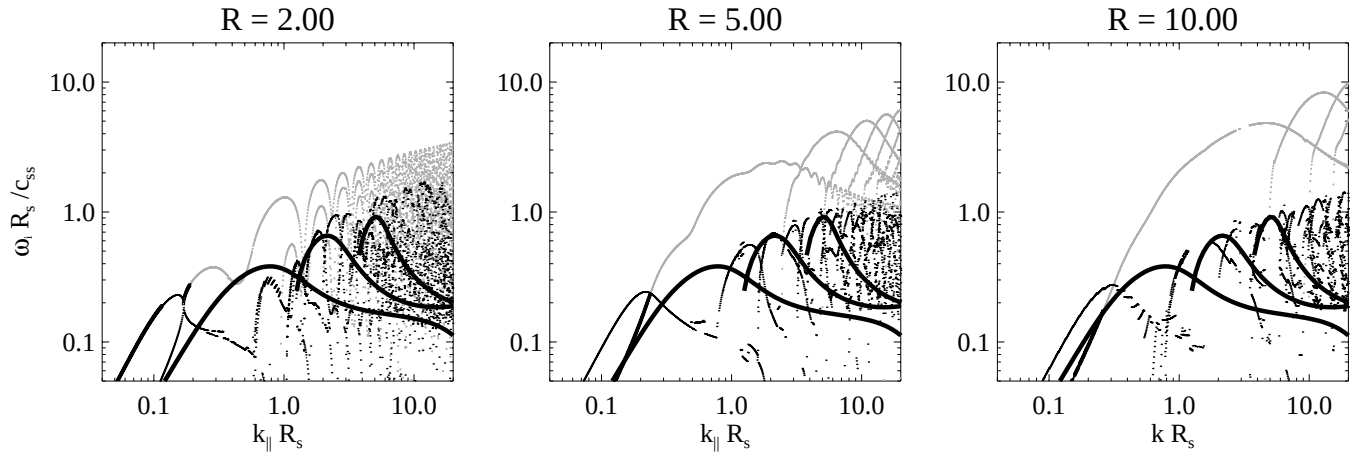

Fig. 2. The solutions (growth rate) of single sheet-external jet with parameters $M_s = 3, \eta_{se} = 0.1$ as in Fig. 1, (thick, black lines) on the background of the stratified jet solutions of Fig. 1. Note, the choice of R-values is slightly different than in Fig. 1.

1985) with phase velocity equal to the bulk velocity of the sheet. Distortion of the pattern for frequency solutions at the transition between core and sheet modes extends the existence of this kind of waves towards small wavelengths too. Such waves are standing in the reference frame of the sheet ie. they are not acoustic waves. They are also not propagating in the direction perpendicular to the jet axis, so the term 'reflection' is not applicable (however, formally the reflection coefficients entering our classification can be computed).

3.5. The case of slower core

Up to now, we presented solutions for one given set of parameters, which illustrates the complexity of the linear analysis and provides a good qualitative description for a wide range of parameters. We did not perform a complete study of all possible parameters range, but restrict ourselves to a few cases which could illustrate different qualitative behavior. Here we want to describe briefly the result obtained for the case of stratified jets with core propagating slower than sheet, which can be generated in some cases of centrifugal acceleration of MHD jets (see eg. Koide et al. 1998)

We consider the same parameters as in Fig. 1, except that now $M_c = 3$ and $M_s = 10$. The global pattern of the solutions appear somewhat comparable to the previous case, with similar maximal growth rates. The solutions can be again classified into three modes, however contrary to the former case, now the modes of the type (a) are absent and the modes of type (d) takes their place in the whole analysis. The exclusive reflection of waves internal to the core on the *cs*-boundary (case a) does not provide any unstable modes.

4. Discussion and conclusions

It is difficult to confront directly the results of this linear analysis to observed jets where non linear effects are likely to be important. However we can consider that the non-linear phase of instability evolution will lead to the formation of shocks at regular spacing corresponding to the wavelength of the fastest growing modes, as observed in the numerical simulations of hydrodynamic supersonic jets by Bodo et al, 1994. Such shocks may have a chance to be observed as they can locally enhance the electromagnetic emission. A complex pattern could result since the propagation angle of the waves and hence the orientation of the shocks fronts is not the same in the core and in the sheet. This seems to be beyond the sensitivity and resolution of present telescopes for the majority of observable radio jets, except perhaps in the case of M87. Indeed recent data show significant evidence for the presence of different layers as a function of distance from the axis in the inner jet of this radiogalaxy. The optical emission is concentrated on the jet axis. It shows oscillations of the jet ridge-line and fast apparent motion. On the other hand, the radio emission is limb brightened and possibly concentrated in the outer jet layers. It shows possible oblique shocks or helical structures, and no apparent motion on similar scales (Biretta, 1996). The stratified jet scenario appears quite relevant to give account for the observed radial structure and for the complexity of the morphology and velocity field in this source.

It could also provide some direct explanation of the complex velocity fields observed in the superluminal quasar 3C345 where two types of components, strong and weak, have been found in the jet. The weak component are much slower and less luminous than the strong ones. We have shown in this paper that several types of waves corresponding to different modes and different propagation velocities can develop in a stratified jet. Thus it is tempting to ascribe the strong jet components to the modes representing the core modes or with longitudinal phase speed related to the core speed and the weak jet components to the modes representing the sheet modes or with longitudinal phase speed related to the sheet speed. In the frame of linear instability model this would nicely explained why, although of different nature, strong and weak components can be related to the same outbursts of the nucleus, observed in 1982 for strong components C3, C3a, C4 and weak component C5, and in 1992 for strong component C7 and weak component C6 (Lobanov,

Zensus, 1996). One basic difficulty with such kind of proposal (but this is the same problem for single non-stratified jets) is that non linear saturation of the Kelvin-Helmholtz instability may prevent the formation of detectable features in relativistic jets (Hanasz, 1995, 1997; Duncan, Hughes, 1994; Marti et al, 1997; Nishikawa et al, 1997).

Our analysis shows that the linear Kelvin-Helmholtz instability of stratified jets is not a simple superposition of solutions of dispersion relations treated independently for the core and the sheet. The presented solutions display a nontrivial interplay of the sheet and core instabilities.

For smaller sheet radii, the growth rate and the wavenumber of the most unstable perturbation are on the sheet modes comparable, although usually smaller than for the core modes. This does not mean that the sheet branch is less relevant. One can expect a similar relation as between the fundamental and the reflection modes in the case of single jets. The relevance of the long less unstable wavelengths relies on the fact that the short wavelength modes have a tendency to saturate at much smaller amplitudes than the long wavelength modes, due to the non-linear effects. The long wavelength, less unstable modes are on the other hand more disruptive as it follows from numerical simulations (eg. Norman and Hardee, 1988).

We notice that while the growth rate for the sheet modes is comparable to the case of single sheet-external jet, the core modes are much more unstable. It is remarkable that the difference between the growth rate of core modes and sheet modes (or single sheet-external modes) is more and more significant when the sheet radius grows. Clearly, the core and sheet modes should not be interpreted as the instability of the core and sheet components exclusively, but as the instability of the entire stratified jet configuration. *Then, we can conclude that the Kelvin-Helmholtz instability of a jet is enhanced at the linear stage by the injection of an internal core component.* Although we did not explore widely the parameter space we expect that this result is quite general. To justify this expectation we note that the dynamical time scale (the sound crossing time) is in the core typically shorter than in the sheet because of (i) the smaller radius and (ii) the typically larger sound speed than in the sheet. The presence of a smaller scale inner component can therefore destabilize the large scale flow due to the much faster time-scale of growth of the instability in the stratified scenario.

Acknowledgements. This project was partially supported by the "Jumelage" program for Polish-French collaboration and the post-doctoral fellowship (MH) from the French Minister of Research, Education and Technology. We thank R. Grappin, J.M. Ibanez, J. Léorat, J.M. Marti and L. Rudnick for discussions.

References

Bahcall, J.N., Kirhakos, S., Schneider, D.P. et al.,1995, ApJ, 452, L91
Balick, B. Icke, V., Mellema, G., 1998, in Williams, B., STScI Newsletter, 15 (1), p2 (HST-NASA).
Balick, B, Perinotto, M., Maccioni, A., Terzian, Y., Hajian, A, 1994, ApJ, 424, 800
Begelman, M.C., McKee, C.F., 1983, ApJ, 271, 89
Biretta, J.A., 1996, Energy transport in radio galaxies and quasars, P.E. Hardee, A.H. Bridle, J.A. Zensus, eds, A.S.P. Conf. Ser. vol 100, p. 187
Bodo, G., Massaglia, S., Ferrari, A., Trussoni, E., 1994, A&A, 283, 655
Cernicharo, J., Neri, R., Reipurth, B., 1997, Herbig-Haro flows and the birth of low mass stars, Reipurth, B., Bertout, C., eds, Kluwer Academic Publisher (IAU Symposium 182), p. 141
Corradi, R.L.M., Schwarz, H.E., 1993a, Stellar jets and bipolar outflows, Errico L., Vittone, A.A., eds, Kluwer Academic Publisher, p. 215
Corradi, R.L.M., Schwarz, H.E., 1993b, A&A, 278, 247
Duncan, G.C., Hughes, P.A., 1994, ApJ, 436, L119
Emmering, R.T., Blandford, R.D., Shlosman, I., 1992, ApJ, 385, 460
Ferreira, J., Pelletier, G., Appl, S., 1997, in Low Mass Star Formation - from infall to outflow, poster proceedings of IAU Symp. 182, Malbet, F., Castets, A., eds, Observatoire de Grenoble, p. 112
Ferrari, A., Trussoni, E., Zaninetti,L., 1978, A&A , 64, 43
Ferrari, A., Trussoni, E., Zaninetti,L., 1982, MNRAS, 198, 1065
Glatzel, W., 1989, J. Fluid Mech., 202, 515
Goodson, A.P., Winglee, R.M., Bőhm, K.-H., 1997, ApJ, 489, 199
Guilloteau, S., Dutrey, A., Gueth, F., 1997, Herbig-Haro flows and the birth of low mass stars, Reipurth, B., Bertout, C., eds, Kluwer Academic Publisher (IAU Symposium 182), p. 365
Hajian, A.R., Balick, B., Terzian, Y., Perinotto, M., 1997, ApJ, 487, 304
Hanasz, M. 1995, PhD Thesis, Nicolaus Copernicus University, Toruń
Hanasz, M., 1997, Relativistic jets in AGNS, Ostrowski, M., Sikora, M., Madejski, G., Begelman, M., eds, Krakow, p. 85
Hanasz, M., Sol, H., 1996, A&A, 315, 355 (Paper I)
Hardee, P.E., Norman, M.,L., 1988, ApJ , 334, 70
Hartigan, P., Morse, J.A., Heathcote, S., Cecil, G., 1993, ApJ, 414, L121
Hutchings, J.B., Crenshaw, D.M., Kaiser, M.E. et al., 1998, ApJ, 492, L115
Koide, S., Shibata, K., Kudoh, T., 1998, ApJ Lett, 495, L63
Kwan, J., Tademaru, E., 1988, ApJ, 332, L41
Kwan, J., 1997, Herbig-Haro flows and the birth of low mass stars, Reipurth, B., Bertout, C., eds, Kluwer Academic Publisher (IAU Symposium 182), p. 443
Lobanov, A.P., Zensus, J.A., 1996, Energy transport in radio galaxies and quasars, P.E. Hardee, A.H. Bridle, J.A. Zensus, eds, A.S.P. Cof. Ser. vol 100, p. 109
Marti, J.M., Müller, E., Font, J.A., Ibanez, J.M., Marquina, A., 1997, ApJ, 479, 151
Nishikawa, K.-I., Koide, S., Sakai, J.-I. et al., 1997, ApJ, 483, L45
Norman, M.,L., Hardee, P.E., 1988, ApJ , 334, 80
Padman, R., Lasenby, A.N., Green, D.A., 1991, Beams and jets in Astrophysics, Hughes, P.A., ed, Cambridge University Press, p. 484
Payne, D.G., Cohn, H., 1985, ApJ, 291, 655.
Press, W.H., Flannery, B.P., Teukolsky, S.A., Vetterling, W.T., 1992, *Numerical recipes*, Cambridge University Press.
Ray, T.P., Mundt, R., 1993, Astrophysical jets, Burgarella, D., Livio, M., O'Dea, C.P., eds, Cambridge University Press, p. 145
Reipurth, B., Heathcote, S., 1993, Astrophysical jets, Burgarella, D., Livio, M., O'Dea, C.P., eds, Cambridge University Press, p. 35
Rudnick, L., Katz-Stone, D., 1996, Energy transport in radio galaxies and quasars, P.E. Hardee, A.H. Bridle, J.A. Zensus, eds, Astronomical Society of the Pacific Conference Series Volume 100, p. 233

Sahai, R., Hines, D.C., Kastner, J.H., Weintraub, D.A., Trauger, J.T., Rieke, M.J., Thompson, R.I., Schneider, G., 1998a, ApJ, 492, L163
Sahai, R., et al, 1998b, ApJ, 493, 301
Schwarz, H.E., Aspin, C., Corradi, R.L.M., Reipurth, B., 1997, A&A, 319, 267
Shu, F., Najita, J., Ostriker, E., Wilkin, F., Ruden, S., Lizano, S., 1994, ApJ, 429, 781
Shu, F.H., Shang, H., 1997, Herbig-Haro flows and the birth of low mass stars, Reipurth, B., Bertout, C., eds, Kluwer Academic Publisher (IAU Symposium 182), p. 225
Solf, J., 1993, Stellar jets and bipolar outflows, Errico L., Vittone, A.A., eds, Kluwer Academic Publishers, p. 145
Solf, J., 1997, Herbig-Haro flows and the birth of low mass stars, Reipurth, B., Bertout, C., eds, Kluwer Academic Publisher (IAU Symposium 182), p. 63
Stahler, S.W., 1993, Astrophysical jets, Burgarella, D., Livio, M., O'Dea, C.P., eds, Cambridge University Press, p. 183
Synge, J.L., 1957, *The relativistic gas*, North-Holland Publishing Company.